A STOCHASTIC LAGRANGIAN MODEL FOR NEAR-WALL TURBULENT HEAT TRANSFER

Sandip Mazumder
and
Michael F. Modest

Department of Mechanical Engineering,
The Pennsylvania State University,
University Park, PA 16802.

Abstract

The modeling of near-wall turbulent heat transfer necessitates appropriate description of near-wall effects, namely, molecular transport, production of turbulence by inhomogeneities, and dissipation of the temperature fluctuations by viscosity. A stochastic Lagrangian model, based on the velocity-composition joint probability density function (PDF) method, has been proposed. The proposed model, when compared with experimental and direct numerical simulation (DNS) data, overdamps the dissipation of the temperature fluctuations in the inertial sublayer, but reaches the correct limit at the wall. The performance of the model has also been compared to the standard k-ϵ and the algebraic Reynolds stress model (ARSM) for both constant heat flux and constant temperature boundary conditions at large Reynolds numbers. The Lagrangian nature of the model helps eliminate numerical diffusion completely.

Nomenclature

a_i, b_i, c_i	arbitrary constants in asymptotic expansion
A	constant in thermal wall-function
C_p	specific heat capacity at constant pressure
C_μ	constant in turbulence model
$f_{u\phi}$	velocity-composition joint PDF
H	channel half-height
k	turbulent kinetic energy
n	time index
Pr	Prandtl number
Pr_t	turbulent Prandtl number
q_w	wall heat flux
$\overline{q}_w$	nondimensional wall heat flux
R_i	standardized Gaussian random number
R_{vT}	notation for $\overline{u_2' T'} \,/\, u_\star \, T_\star$
Re_H	Reynolds number based on channel half-height
t	time
T	instantaneous Eulerian temperature
T_i	inlet bulk temperature
$\overline{T}$	mean Eulerian temperature

$T^\star$	Lagrangian temperature
T'	temperature fluctuations
T_w	wall temperature
$T_\star$	wall conduction temperature
$\overline{U}_i$	mean Eulerian velocity in the i-th direction
u_i'	velocity fluctuation in the i-th direction
$U_i^\star$	Lagrangian velocity in the i-th direction
$\underline{U}$	instantaneous Eulerian velocity vector
$u_\star$	friction velocity
W_i	isotropic Wiener process
x_i	space variable
$x_i^\star$	position vector of a particle
x_{2+}	x_2 normalized by $\nu \,/\, u_\star$

Greek

α_H	thermal diffusivity
δ_{ij}	Kronecker delta
ϵ	rate of dissipation of k
κ	Von Karman constant
ν	kinematic viscosity
ϕ	arbitrary passive scalar
θ_T, θ_q	nondimensional temperature
θ_m	nondimensional bulk temperature
θ_w	nondimensional wall temperature
θ^+	root-mean-square temperature fluctuation normalized by $T_\star$
ρ	density
τ	turbulent time-scale
τ_ϕ	time scale for scalar dissipation

Introduction

The velocity-composition joint PDF method (Pope, 1985) is an important tool for the computation of turbulent reactive flows. Starting with the conservation equations for mass, momentum, energy, and concentrations of various species (for chemically reactive flows), a single transport equation can be derived for the joint probability density function of velocity and composition, $f_{u\phi}(\underline{V}, \underline{\psi}; \underline{x}, t)$, as described by Pope (1985). The quantity $f_{u\phi}\, d\underline{V}\, d\underline{\psi}$ represents the probability that $\underline{V} \le \underline{U} \le \underline{V}+d\underline{V}$ and $\underline{\psi} \le \underline{\Phi} \le \underline{\psi} + d\underline{\psi}$ occur simultaneously, where $\underline{U}$ is the velocity vector, $\underline{\Phi}$ is the set of all scalars (temperature or enthalpy, and concentrations), and $\underline{V}$ and $\underline{\psi}$ are independent sample-space variables corresponding to $\underline{U}$ and $\underline{\Phi}$, respectively. The transport equation for the joint PDF is a multi-dimensional partial differential equation, and cannot be solved efficiently by traditional finite-difference or finite-volume techniques, and the Monte-Carlo method is used instead. In this method, the fluid within the whole computational domain is discretized into representative 'particles' (or samples). These 'particles' then move with time and their motion is governed by their Lagrangian momentum equations, which are recast in such a way that the forces acting on these representative

'particles' are modeled after stochastic processes. The detailed equations for particle transport may be found in Pope (1985). The particles carry with them all passive scalars, as well, and transport of energy will be discussed in this article.

During the last two decades, the velocity-composition joint PDF method has been used effectively to predict hydrodynamic and scalar fields in free-shear flow situations, namely, jet flames, mixing layers, and wakes (Janicka *et al.*, 1978; Lockwood and naguib, 1975; Anand and Pope, 1987; Haworth and Pope, 1987). Recently, the method has been applied to wall-bounded isothermal inert flows by Mazumder and Modest (1996) and by Dreeben and Pope (1995). The method has yet to be applied to scalar transport in near-wall regions of a turbulent flow. This article describes a methodology for incorporating scalar transport using the velocity-composition joint PDF method to wall-bounded turbulent flows.

Exact Lagrangian Description

In near-wall regions in a turbulent flow, two very important effects come into play. First, molecular transport starts to dominate as the wall is approached. Secondly, the turbulent fluctuations, which are primarily generated in the inertial sublayer due to non-linear interactions, are completely damped out by viscosity in the viscous sublayer. The first of these two effects can be treated exactly by deriving the exact Lagrangian equation for a fluid particle. The second effect will be discussed in detail in a later section.

Consider a fluid particle moving through space with position $x_i^\star(t)$, velocity $U_i^\star(t)$, and temperature $T^\star(t)$. This is the Lagrangian description of the fluid particle. The Lagrangian temperature, $T^\star(t)$, is related to the Eulerian temperature field, $T(x_i\,,\,t)$, by the relationship

$$T_i^\star(t) \;=\; T\,[x_i = x_i^\star(t)\,,\,t]\,. \tag{1}$$

The increment in temperature of a particle, $\Delta T^\star$, over a time Δt may be obtained by performing a Taylor series expansion:

$$\Delta T^\star \;=\; \frac{\partial T}{\partial t}\,\Delta t \;+\; \frac{\partial T}{\partial x_i}\,\Delta x_i^\star \;+\; \frac{1}{2}\,\frac{\partial^2 T}{\partial x_i\,\partial x_j}\,\Delta x_i^\star\,\Delta x_j^\star \;+\; \ldots \tag{2}$$

where the second-order temporal term has been neglected because later on, only a first-order accurate time-marching scheme will be used to solve the final governing equations. If a particle is introduced into a fluid stream, it will be convected along the stream according to the Lagrangian equation

$$\Delta x_i^\star \;=\; U_i^\star\,\Delta t \;=\; U_i\,[x_i = x_i^\star(t)\,,\,t]\,\Delta t\,. \tag{3}$$

In the absence of convective transport, the particle could move by molecular mechanisms alone. At large Reynolds numbers, these molecular transport forces are very weak compared to the convective forces, and are typically neglected. In regions close to the wall, these forces become large, and need to be included. Einstein (1926), during his studies on Brownian motion, first suggested from a stochastic viewpoint that a particle in a stagnant fluid would move following the equation

$$\Delta x_i^\star \;=\; \sqrt{2\,\nu}\;\Delta W_i\,, \tag{4}$$

where W_i is an isotropic Wiener process, and ν is the kinematic viscosity of the fluid. The Wiener process is a non-differentiable function, which, when integrated over time, yields a random number

drawn from a standardized Gaussian distribution with zero mean and a variance equal to the time interval over which the integration has been performed. For details pertaining to the Wiener process and other stochastic processes and terminology, the readers are referred to the two texts by Karlin and Taylor (1975,1981). In the presence of both convection and molecular transport, the increment of a particle's position would be expressed as

$$\Delta x_i^\star \;=\; U_i^\star \, \Delta t \;+\; \sqrt{2\,\nu}\;\Delta W_i \;. \tag{5}$$

In addition to the aforestated properties, the Wiener process also has the following property (Einstein, 1926):

$$\overline{\Delta W_i \, \Delta W_j} \;=\; \delta_{ij} \, \Delta t \;, \tag{6}$$

where δ_{ij} is the Kronecker delta. Substituting equation (5) and (6) into equation (2), and retaining terms up to order Δt, we have

$$\Delta T^\star \;=\; \frac{\partial T}{\partial t}\,\Delta t \;+\; \frac{\partial T}{\partial x_i}\,(U_i^\star \, \Delta t \;+\; \sqrt{2\,\nu}\;\Delta W_i) \;+\; \nu\,\frac{\partial^2 T}{\partial x_i \, \partial x_i}\,\Delta t \;. \tag{7}$$

In the absence of chemical reaction, and neglecting viscous dissipation, radiation and pressure-work, for constant thermophysical properties, the instantaneous Eulerian energy transport equation is given by:

$$\frac{\partial T}{\partial t} \;+\; U_i\,\frac{\partial T}{\partial x_i} \;=\; \alpha_H\,\frac{\partial^2 T}{\partial x_i \, \partial x_i} \;, \tag{8}$$

where α_H is the thermal diffusivity of the fluid, and is expressed as

$$\alpha_H \;=\; \lambda \,/\, \rho \, C_p \;, \tag{9}$$

where λ is the thermal conductivity, ρ is the density, and C_p is the specific heat capacity at constant pressure. Substitution of equations (3) and (8) into equation (7) yields

$$\Delta T^\star \;=\; (\alpha_H \;+\; \nu)\,\frac{\partial^2 T}{\partial x_i \, \partial x_i}\,\Delta t \;+\; \sqrt{2\,\nu}\;\Delta W_i\,\frac{\partial T}{\partial x_i} \;. \tag{10}$$

Equation (10) is the exact Lagrangian energy transport equation for a fluid particle, whose molecular motion has been modeled after a stochastic process. The instantaneous Eulerian temperature can be decomposed into its mean and fluctuating parts and used in equation (10) to yield

$$\Delta T^\star \;=\; (\alpha_H \;+\; \nu)\,\frac{\partial^2 \overline{T}}{\partial x_i \, \partial x_i}\Delta t \;+\; \sqrt{2\,\nu}\;\Delta W_i\,\frac{\partial \overline{T}}{\partial x_i} \;+\; (\alpha_H \;+\; \nu)\,\frac{\partial^2 T'}{\partial x_i \, \partial x_i}\Delta t \;+\; \sqrt{2\,\nu}\;\Delta W_i\,\frac{\partial T'}{\partial x_i} \;, \tag{11}$$

where the overbars denote Eulerian mean quantities, and the primes denote fluctuations. The first two terms can be calculated exactly by averaging over Monte-Carlo cells and then by fitting splines as described by Mazumder and Modest (1996). The last two terms need to be modeled for complete closure.

Deterministic Model for Fluctuations

To model velocity fluctuations, the Langevin model can be used effectively. The same model, however, causes unboundedness of scalars such as temperature (Pope, 1985). The temperature-space, unlike velocity-space, is a bounded sample-space, the bounds being provided by the Second Law of Thermodynamics. The Langevin model does not take this constraint into account and, therefore, cannot be used to model temperature fluctuations. In the seventies, Dopazo (1975) proposed a deterministic model for scalar fluctuations in homogeneous turbulence. His model is expressed as:

$$\frac{d\phi^\star}{dt} \;=\; -\frac{1}{2}\,\frac{1}{\tau_\phi}\,(\phi^\star \;-\; \overline{\phi})\,, \tag{12}$$

where ϕ is any passive scalar, and τ_ϕ is the time-scale for the dissipation of scalar fluctuations. In homogeneous turbulence, the first two terms on the right-hand-side of equation (11) are absent and consequently, equation (12) is actually a model for the last two terms on the right-hand-side of equation (11). Equation (12), upon multiplication by $\phi' \;=\; \phi^\star \;-\; \overline{\phi}$, and some manipulation, yields

$$\frac{d\overline{\phi'^2}}{dt} \;=\; -\frac{1}{\tau_\phi}\,\overline{\phi'^2}\,. \tag{13}$$

The above model, when used for the temperature, suggests that the mean-square temperature fluctuations will decay exponentially with time in homogeneous turbulence. In regions close to the wall, the time-scale, as well as the mean temperatures, are strong functions of space, and need to be modified. This can be achieved by using thermal wall-functions and scaling arguments.

Consider a wall lying on the x_1-x_3 plane, and let x_2 be the normal distance from the wall. The predominant flow direction is x_1 and x_3 is the azimuthal direction in which gradient of all mean quantities are zero. For such a case, in the inertial sublayer, the mean temperature is given by the expression (White, 1991)

$$\overline{T} \;=\; T_w \;-\; \frac{q_w}{\rho\, C_p\, u_\star}\,\left[\frac{\mathrm{Pr}_t}{\kappa}\,\ln\left(\frac{x_2\, u_\star}{\nu}\right) \;+\; A\right]\,, \tag{14}$$

where T_w is the wall temperature, q_w is the wall heat flux based on the thermodynamic sign convention, and Pr_t is the turbulent Prandtl number. κ, the Von Karman constant, is equal to 0.42, and $u_\star$ is the friction velocity, given by (Launder *et al.*, 1984)

$$u_\star \;=\; C_\mu^{1/4}\, k^{1/2}\,, \tag{15}$$

where k is the turbulent kinetic energy, and C_μ is equal to 0.09. The parameter A, in equation (14), is a function of the Prandtl number of the fluid (Kader, 1981):

$$A \;=\; (3.85\,\mathrm{Pr}^{1/3} \;-\; 1.3)^2 \;+\; 2.12\,\ln(\mathrm{Pr})\,, \tag{16}$$

where Pr is the Prandtl number. In the viscous sublayer the mean temperature is given by

$$\overline{T} \;=\; T_w \;-\; \frac{q_w}{\rho\, c_p\, u_\star}\,\left[\mathrm{Pr}\,\left(\frac{x_2\, u_\star}{\nu}\right)\right]\,. \tag{17}$$

Several authors have suggested that the time-scale for scalar dissipation, τ_ϕ, is linearly proportional to the turbulent time-scale, τ. Beguier *et al.* (1978) suggested that the ratio of these two time-scales, $C_\phi = \tau / \tau_\phi$, assumes a value close to 2.0 for most shear flows. Experiments performed by Warhaft and Lumley (1978) suggest that C_ϕ is not a universal constant. Warhaft (1980) suggested values of C_ϕ in the range between 1.9 and 3.1. This is still a topic of turbulence research, and will not be dwelt upon further in this article. For the current study a value of 2.0 was used. The turbulent time-scale, τ, is actually the time-scale for the dissipation of turbulent kinetic energy, and is given by the ratio, k / ϵ, where ϵ is the rate of dissipation of the turbulent kinetic energy. In inhomogeneous turbulence, the time-scale is a function of space, and changes rapidly close to solid walls. In the near-wall layer, a good estimate of the dissipation rate is given by (Tennekes and Lumley, 1967)

$$\epsilon = u_\star^3 / \kappa x_2 , \tag{18}$$

which upon combination with equation (15) and the use of the definition of the turbulent time-scale yields

$$\frac{1}{\tau} = \frac{C_\mu^{3/4} k^{1/2}}{\kappa x_2} . \tag{19}$$

It is useful at this point to investigate the modeled behavior of the temperature fluctuations as a function of the distance from the wall. In order to do that, we express velocity and temperature fluctuations as arbitrary functions of distance normal to the wall, x_2, yielding

$$u_i' = a_i + b_i x_2 + c_i x_2^2 + \ldots ,$$

and

$$T' = a_T + b_T x_2 + c_T x_2^2 + \ldots , \tag{20}$$

where a_i, b_i, c_i, a_T, b_T, and c_T are all arbitrary functions of x_1, x_3 and t. Application of no-slip, continuity, and zero temperature fluctuation at the walls yield:

$$\begin{aligned} u_1' &= b_1 x_2 + c_1 x_2^2 + \ldots , \\ u_2' &= c_2 x_2^2 + \ldots , \\ u_3' &= b_3 x_2 + c_3 x_2^2 + \ldots , \end{aligned}$$

and

$$T' = b_T x_2 + c_T x_2^2 + \ldots . \tag{21}$$

Equation (12), when written for temperature, and using $C_\phi = \tau / \tau_\phi$, yields

$$\frac{dT^\star}{dt} = -\frac{C_\phi}{2\,\tau} (T^\star - \overline{T}) . \tag{22}$$

The wall functions, which we are using here [equations (14) and (17)], suggest that the mean temperature, $\overline{T}$, is only a function of x_2 and therefore, for the near-wall region, equation (22) may

be written as

$$\frac{dT'}{dt} = \frac{dT'}{dx_2^\star}\frac{dx_2^\star}{dt} = U_2^\star \frac{dT'}{dx_2^\star} = -\frac{C_\phi T'}{2\tau}, \tag{23}$$

where $T' = T^\star - \overline{T}$ represents the deviation of the particle temperature from the mean, and $U_2^\star$ is the particle velocity in the direction normal to the wall. The particle velocity normal to the wall is a sum of the mean velocity and a fluctuation, both normal to the wall. Application of no-slip and continuity easily reveals that the mean normal velocity, $\overline{U}_2$, is zero in the near-wall region. The use of equation (21) for the normal velocity fluctuation yields

$$U_2^\star = c_2 x_2^{\star 2} + \mathcal{O}(x_2^{\star 3}). \tag{24}$$

The coefficient, c_2, will be negative if a particle moves toward a wall, and positive if it moves away from a wall. According to equation (24), if a particle travels toward the wall, its velocity (and consequently, the normal velocity fluctuation) will decrease monotonically, until it reaches the wall, where its velocity will be zero. This is not the correct picture, as shown earlier by Mazumder and Modest (1996). The particle's normal velocity actually reaches zero and changes sign even before the wall is reached. This, however, can only be obtained by solving a system of ordinary differential equations for particle motion, taking all physical processes into account. For the current purposes, equation (24) gives a reasonable functional behavior of the normal velocity, especially since it does not violate any conservation laws or boundary conditions. Substituting equations (19) and (24) into equation (23), and retaining terms up to leading order yields

$$\frac{dT'}{dx_2^\star} = -\frac{C_\phi\, T'\, C_\mu^{3/4}\, k^{1/2}}{2\, c_2\, \kappa\, x_2^{\star 3}}. \tag{25}$$

Using $k = \overline{u_i' u_i'}\,/\,2$, and equation (21), it can be shown that up to leading order,

$$k = \frac{(\overline{b_1^2} + \overline{b_3^2})}{2} x_2^2, \tag{26}$$

which upon substitution into equation (25) yields

$$\frac{dT'}{dx_2^\star} = -\frac{C_\phi\, C_\mu^{3/4}\,(\overline{b_1^2} + \overline{b_3^2})\, T'}{4\, c_2\, \kappa\, x_2^{\star 2}} = -C\,\frac{T'}{x_2^{\star 2}}, \tag{27}$$

where the constant C has been introduced for brevity. Following the sign of c_2, the constant C will be negative for a particle moving towards the wall, and positive for a particle moving away from the wall. Integration of equation (27) from a given normal location $x_{2,0}^\star$, where the fluctuation is T_0', to an arbitrary location along a particle path, yields

$$T' = T_0' \exp\left[C\left(\frac{1}{x_2^\star} - \frac{1}{x_{2,0}^\star}\right)\right] \tag{28}$$

Obviously, the modeled behavior of the temperature fluctuations near the wall, shown in equation (28), is different from the modeled behavior shown by the asymptotic expansion in equation (21). The level of disparity will depend largely on the unknown coefficients. It should also be noted that

the above analysis only accounted for dissipation of the fluctuations by viscosity. It did not account for transport or production of the fluctuations. In spite of all this, it reveals one very important characteristic of the proposed model: in the limiting case of $x_2^\star \rightarrow 0$, the temperature fluctuations are zero. This simple observation may appear trivial. However, it is not so in the context of Lagrangian schemes and models. The proposed model [equation (22)] is an initial value problem in time, and not a boundary value problem in space, where spatial boundary conditions can be easily implemented. Therefore, in such Lagrangian formulations, it is not always easy to ensure that certain specific conditions will be satisfied at a certain point in space. In Eulerian schemes, on the other hand, spatial boundary conditions are easily implemented, but instantaneous information pertaining to the fluctuations cannot be obtained. They can only be obtained in an averaged sense.

The problem of damping the turbulent fluctuations at the correct rate near walls has always been a challenge in the field of conventional turbulence modeling. In the past, *ad hoc* damping functions have been used to damp the Reynolds stresses in the viscous sublayer (Hanjalic and Launder, 1976; Launder *et al.*, 1984). Current formulations, such as the one by Durbin (1993), uses an elliptic relaxation technique. For heat transfer, this issue is not usually encountered, simply because of the use of the Reynolds analogy for turbulent transport, which essentially implies that the same damping functions that were used for the Reynolds stresses act to damp the turbulent fluxes, as well. Nevertheless, in light of these problems in Eulerian turbulence models, it is not surprising that Lagrangian models will also be faced with similar problems.

The complete, modeled Lagrangian energy transport equation is obtained by replacing the 'unclosed' terms in equation (11) by the proposed model:

$$\Delta T^\star \;=\; (\alpha_H \,+\, \nu)\,\frac{\partial^2 \overline{T}}{\partial x_i\,\partial x_i}\,\Delta t \;+\; \sqrt{2\,\nu}\,\frac{\partial \overline{T}}{\partial x_i}\,\Delta W_i \;-\; \frac{1}{2}\,\frac{C_\phi}{\tau}\,(T^\star \,-\, \overline{T})\,\Delta t\;. \tag{29}$$

Euler-explicit integration of equation (29) yields

$$T^\star\big|^{n+1} \;=\; T^\star\big|^{n} \,+\, (\alpha_H \,+\, \nu)\,\left.\frac{\partial^2 \overline{T}}{\partial x_i\,\partial x_i}\right|^n \Delta t \,+\, \sqrt{2\,\nu\,\Delta t}\,\left.\frac{\partial \overline{T}}{\partial x_i}\right|^n R_i \,-\, \frac{1}{2}\,\frac{C_\phi}{\tau}\,(T^\star\big|^n \,-\, \overline{T}\big|^n)\,\Delta t\,, \tag{30}$$

where R_i is a random number drawn from a standardized Gaussian distribution with zero mean and variance equal to unity, n is the time-index, and Δt is the time-step. Equation (30) is unstable for large Δt. The stability characteristics can be improved by using $T^\star$ at n + 1 rather than at n in the last term in equation (30). Upon performing that step, we obtain

$$T^\star\big|^{n+1} \;=\; \frac{1}{1 + C_\phi/2\tau}\left[T^\star\big|^n \,+\, (\alpha_H + \nu)\,\left.\frac{\partial^2 \overline{T}}{\partial x_i\,\partial x_i}\right|^n \Delta t \,+\, \sqrt{2\,\nu\Delta t}\,\left.\frac{\partial \overline{T}}{\partial x_i}\right|^n R_i \,+\, \frac{1}{2}\,\frac{C_\phi}{\tau}\,\overline{T}\big|^n \Delta t\right] \tag{31}$$

In the Monte-Carlo simulation, equation (31) is solved along with the hydrodynamic equations of transport. In the near-wall region, since the gradients change rapidly, the same equations, after aforestated modifications, need to be solved using a higher order integration scheme. In the present context, a fourth-order Runge-Kutta method was used. The reader is referred to Mazumder and Modest (1996) for details of the solution algorithm.

Results and Discussion

Validation of Model

Although the primary interest of the authors lies in large Reynolds number flows, data of any reliable nature are not available for Re $> 10^4$. Therefore, validation of the model has been carried out for low Re flows, for which both experimental and DNS data are available. Following this validation, the performance of the model will be compared with conventional turbulence models at high Re.

The test problem considered in this section is the same as the one for which Lyons *et al.* (1991) have provided direct numerical simulation (DNS) data, and Teitel and Antonia (1993) have provided experimental data. A hydrodynamically and thermally fully-developed flow is considered between two parallel plates. The lower plate is heated, while the upper plate is cooled. The thermally fully developed state is attained by ensuring that the same heat flux that is supplied to the bottom plate is removed from the top one. The Reynolds number based on the channel half-height and the bulk-mean flow velocity was chosen as 2262, the same as the one that Lyons *et al.* used for their simulation. Using the properties of air at room temperature and a channel height of 21 mm (used by Teitel and Antonia) gives a bulk-mean velocity of 3.25 m/s. Lyons *et al.* used a Prandtl number of unity for their simulation, while Teitel and Antonia used the Prandtl number of air (= 0.712), which we have chosen to use. Since the results are eventually normalized by the Prandtl number, it is not expected to make a difference, because the Prandtl number appears in a linear form in the governing equations.

The hydrodynamic entry length for the problem under consideration is in the order of hundred times the channel height. To obtain the hydrodynamically fully developed solution, an isothermal case was run for a long channel of a length equal to hundred times the height, with an inlet plug velocity of 3.25 m/s. Such an approach guarantees a bulk-mean velocity of 3.25 m/s. An algebraic Reynolds stress model (ARSM) (Launder *et al.*, 1984) was used as the turbulence model. The velocity profile at the outlet was then used as the inlet profile for an isothermal PDF Monte-Carlo simulation in a channel five times as long as its height. The process of taking the outlet profile and feeding it back as the inlet profile was repeated three times for this shorter channel. This approach was used to eliminate any differences in the fully developed velocity profiles arising due to the differences in the ARSM and the PDF model. Since the problem under consideration is incompressible, once a fully developed hydrodynamic field is reached, it is not violated by any thermal gradients. Therefore, this preprocessed hydrodynamic field was used for the actual simulation, which was performed in a channel twice as long as its height. The thermal simulation was initiated by using the temperature profile provided by the ARSM as a first guess at all axial locations including the inlet. The simulation was repeated thrice after feeding the outlet temperature profile as the inlet, to ensure that all effects of the initial guess was forgotten, and the turbulent statistics provided was indeed one that was simulated by the PDF model.

A 10×80 grid was used for the PDF simulation. Ten points were considered sufficient for the axial direction since both flow and temperature fields are fully developed. In the normal direction, much larger number of sampling bins were used, primarily because the goal of this section is to investigate the performance of the proposed model in near-wall regions. The raw Monte-Carlo data were smoothed using two-dimensional least-square B-splines (DeBoor, 1978). The splines were also used to calculate all required spatial derivatives. The Monte-Carlo simulation was performed with 100,000 particles.

Figure 1 illustrates the behavior of the normalized root-mean-square temperature fluctuations

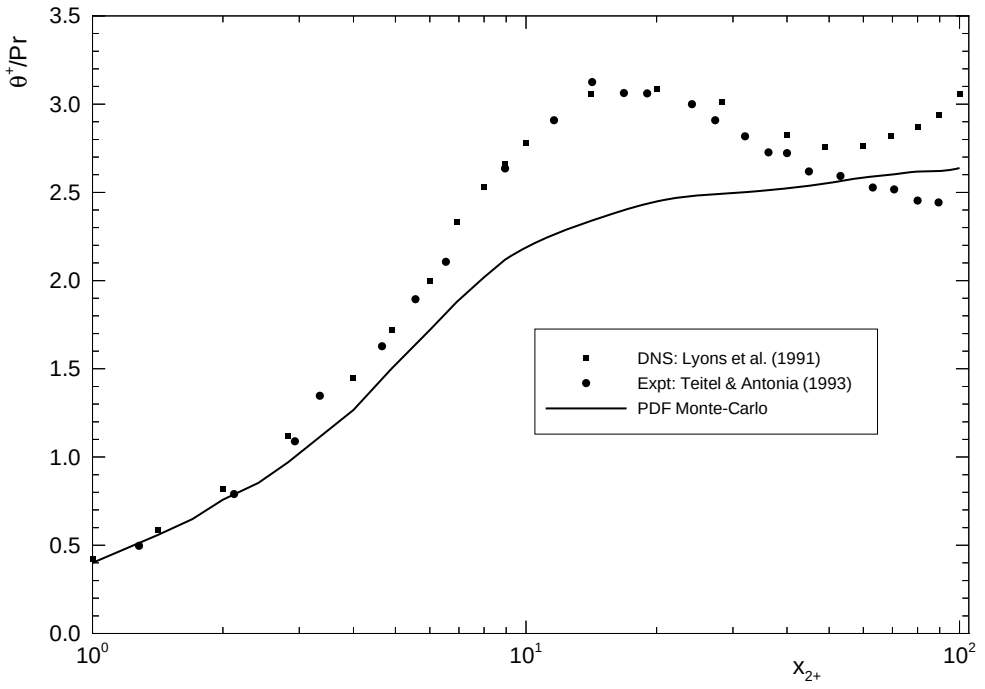

Figure 1: Behavior of root-mean-square temperature fluctuations in near-wall region

near the wall. The notation θ^+ has been used for the quantity $\sqrt{\overline{T'^2}} \,/\, T_\star$, where the wall conduction temperature, $T_\star$, is expressed as

$$T_\star \;=\; \frac{q_w}{\rho\, C_p\, u_\star}\,, \tag{32}$$

where q_w is the supplied wall heat flux. The space variable normal to the wall, x_2, normalized by $\nu/u_\star$, has been denoted by x_{2+}. It is clear that the proposed model overdamps the fluctuations in regions away from the wall *i.e.*, in the inertial sublayer. However, very close to the wall, the correct behavior is replicated. This is consistent with the analytical observations made earlier.

The normalized correlation between the fluctuating normal velocity and the fluctuating temperature has been illustrated in Fig. 2 for the near-wall region. In this case, only DNS data of Lyons *et al.* (1991) have been shown since they match the experimental data of Teitel and Antonia (1993) almost exactly. The quantity $\overline{u_2' T'} \,/\, u_\star\, T_\star$ has been denoted by R_{vT}. In this case, too, the damping rate is overpredicted, but to a smaller degree. This has two probable causes. First, the model used for the velocity fluctuations in the viscous sublayer (Mazumder and Modest, 1996) is quite accurate and accounts for the anisotropic dissipation of the Reynolds stresses. Secondly, since the velocity fluctuation of a particle could correlate positively or negatively with its temperature fluctuation, the error in the prediction of the decay rate of velocity-temperature fluctuations is not exactly proportional to the error in the prediction of the decay rate of the square of the temperature fluctuations.

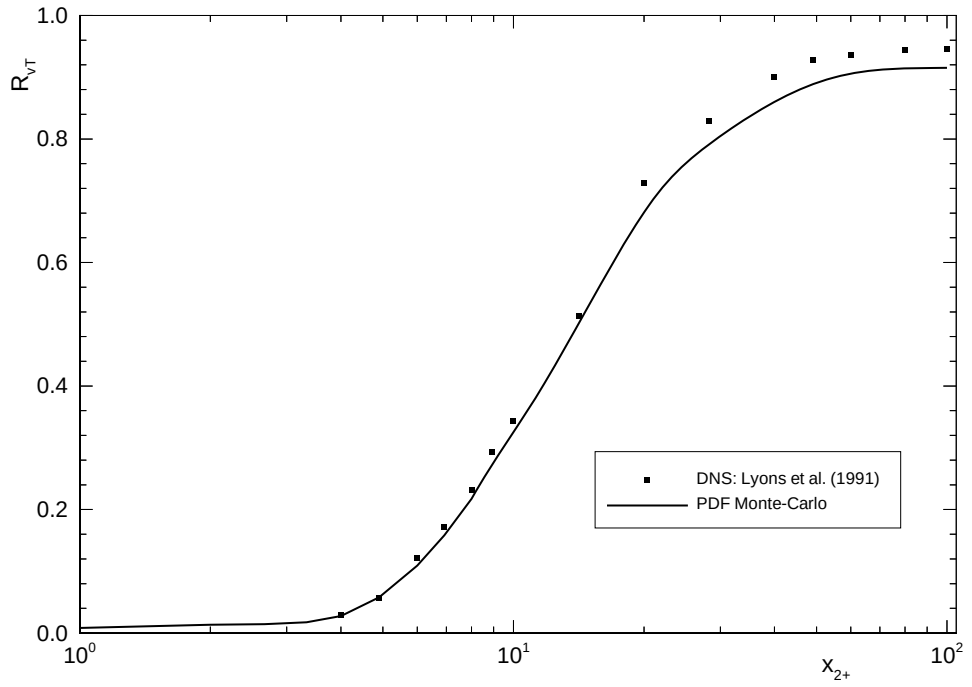

Figure 2: Behavior of normal velocity-temperature correlation in the near-wall region

Comparison with Existing Turbulence Models

The test problem considered for this purpose is that of a thermally developing hydrodynamically fully-developed flow through a channel. The flow is assumed incompressible and two-dimensional in the mean. The channel is 1 m wide and 10 m long. The Reynolds number, based on the channel half-height is, $\mathrm{Re}_H = 5 \times 10^5$. For the sample calculations, a Prandtl number of 0.7 and a turbulent Prandtl number of 0.9 were used. The incoming plug temperature was set to 1000 K. The method was tested for two different boundary conditions: a constant wall temperature boundary condition, with the walls maintained at 300 K, and a constant flux boundary condition, with 1000 W/m^2 rejected at both walls.

The Monte-Carlo calculations, in this case, were performed using 20×10 Monte-Carlo cells and with 100,000 particles. In addition, to account for strong gradients near the wall, the cells adjacent to the walls were broken up into subcells to obtain more samples for spline fitting. The finite-volume k-ϵ / algebraic Reynolds stress (ARSM) (Launder *et al.*, 1984) calculations were performed using the commercial flow code Harwell-FLOW3D with 20×20 finite-volume cells. The thermal wall-functions [equations (14) and (17)] were employed to calculate the wall temperature for the constant wall heat flux case, and to calculate the wall heat flux for the constant wall temperature case.

Figure 3 illustrates nondimensional wall heat fluxes, $\overline{q}_w$, and nondimensional bulk temperatures, θ_m, obtained using the three different models for the case of constant temperature boundary condition. Nondimensional temperatures for the constant temperature boundary condition and the constant heat

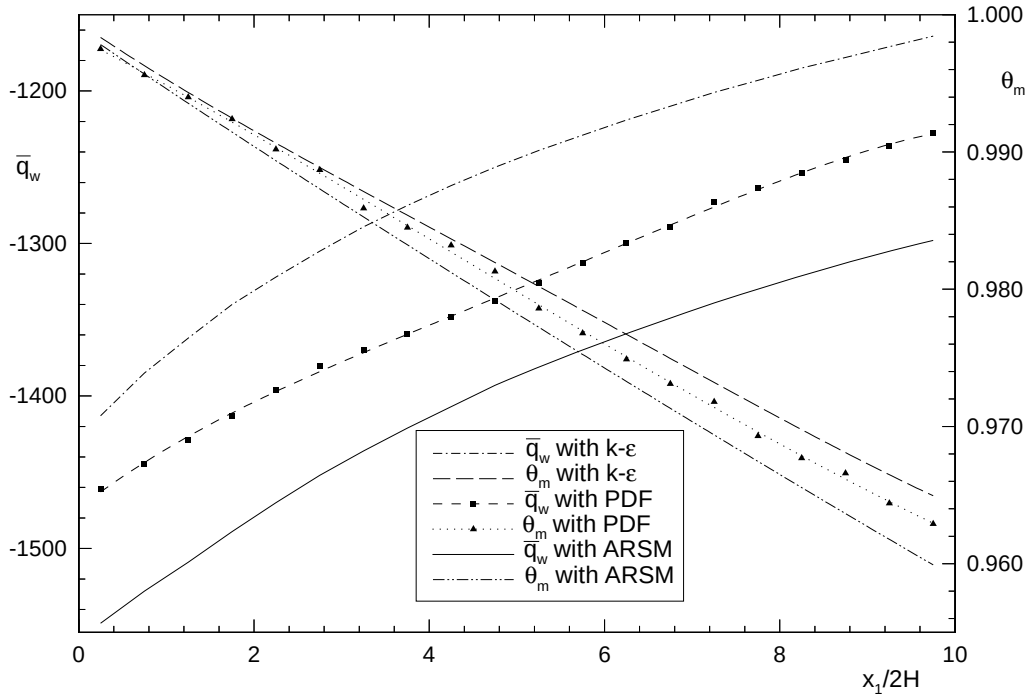

Figure 3: Nondimensional wall heat flux and nondimensional bulk temperature for the case of isothermal walls

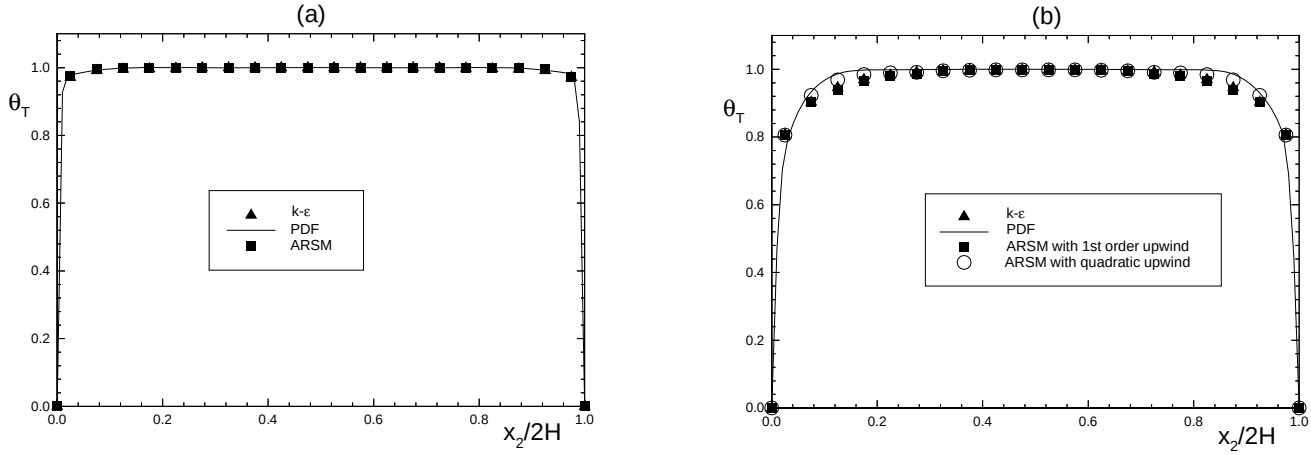

Figure 4: Nondimensional mean temperature profiles for the case of constant wall temperature at (a) $x_1/2\,H$ = 0.25, and at (b) $x_1/2\,H$ = 9.75

flux boundary condition are denoted by θ_T and θ_q, respectively. They are defined as

$$\theta_T \;=\; \frac{\overline{T} \;-\; T_w}{T_i \;-\; T_w} \;;\; \theta_q \;=\; \frac{\lambda\,(T_i \;-\; \overline{T})}{2\,q_w\,H} \;. \tag{33}$$

In the above expressions, T_w is the wall temperature, T_i is the bulk temperature at the inlet, q_w is the wall heat flux, and H is the channel half-height. For the isothermal wall case, the non-dimensional heat flux, $\overline{q}_w$, is defined as

$$\overline{q}_w \;=\; \frac{2\,q_w\,H}{\lambda\,(T_i \;-\; T_w)} \;. \tag{34}$$

The differences in results, obtained by the three methods, is partly due to the use of different turbulent models in the three different cases, and partly due to different numerical techniques used (Lagrangian Monte-Carlo versus Eulerian finite-volume). In k-ϵ and ARSM calculations, the turbulent heat fluxes, $-\rho\,\overline{u_i'\,T'}$, are approximated by using a Gradient Diffusion Hypothesis (Tennekes and Lumley, 1967). However, the hydrodynamic moments are calculated more accurately in the ARSM than in k-ϵ, resulting in different flow fields. The difference in flow fields also led to different temperature fields. In the PDF method, no approximations are made. However, in the PDF method, for purposes of simplicity, a simple algebraic model has been used to calculate ϵ (Mazumder and Modest, 1996), as opposed to the k-ϵ model and ARSM, where the modeled transport equation for ϵ was solved. Figure 4 illustrates the corresponding temperature profiles. The profile obtained by the PDF method was plotted after spline smoothing. Both k-ϵ and the ARSM profiles suffer a 'smearing' effect due to numerical diffusion associated with the use of upwind differencing schemes (Raithby, 1976) at a certain point in space at large Re. The fact that this difference is indeed partly due to numerical diffusion has been demonstrated by using a quadratic upwind differencing scheme (Leshziner, 1980) with the same number of nodes. The effect of numerical diffusion is not observed at the cells adjacent to the inlet because a boundary condition of the first kind is imposed on the upstream face of these cells. The choice of a coarse grid for the PDF method was made to emphasize the point that in spite of the coarse nature of the grid, numerical diffusion problems do not arise in such treatments owing to its Lagrangian nature. For the constant heat flux boundary condition case, the nondimensional wall temperature, θ_w, has been illustrated in Fig.5. The ARSM is observed to predict a somewhat larger wall temperature than the PDF or the k-ϵ model. The bulk temperatures were not plotted because they can simply be obtained from a global energy balance, resulting in the same linear decay in temperature for all three methods. The absence of the non-linear convective terms in the PDF scheme guarantees this global energy balance, as opposed to finite-volume schemes where the satisfaction of the global energy balance may be difficult due to numerical diffusion. The temperature profiles for this case look similar to the ones shown in Fig.4, and have not been shown to save space.

Conclusion

The velocity-composition joint PDF method has been extended to predict the temperature field in an incompressible channel flow. Exact Lagrangian transport equations were derived and solved for this purpose. The temperature fluctuations were modeled using a modified form of an existing model, which was originally developed for homogeneous turbulence. The proposed PDF model overdampens the temperature fluctuations close to the wall, but reaches the correct limiting behavior

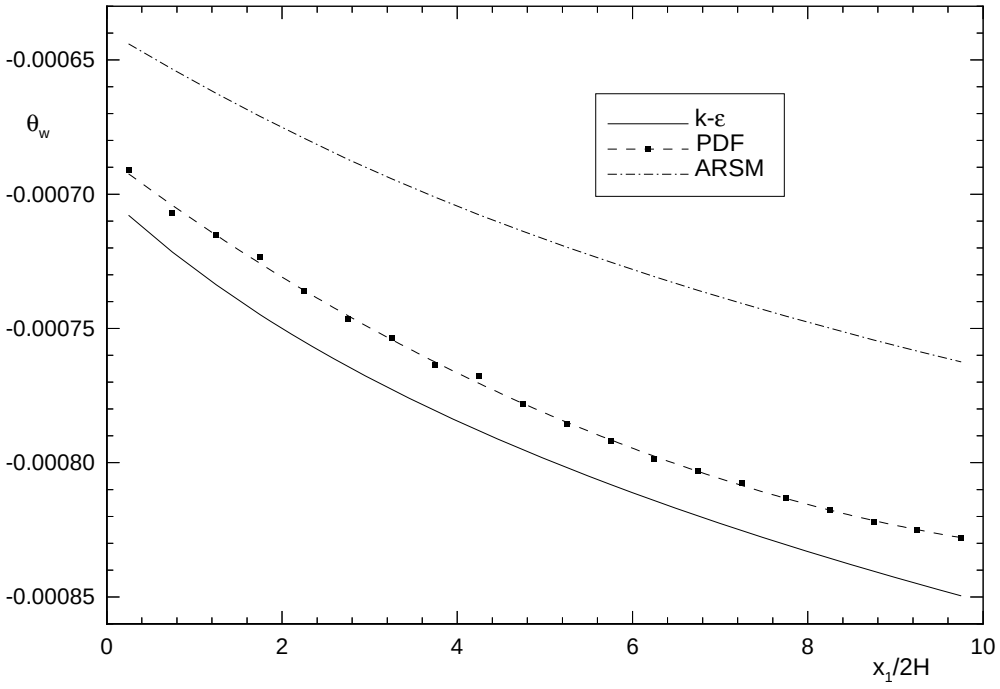

Figure 5: Nondimensional wall temperature for the case of constant heat flux boundary condition

at the wall. This problem, as discussed, is a classical problem in turbulence modeling, and needs further attention and research. The Lagrangian nature of the PDF model helped eliminate numerical diffusion completely. This is a particularly great advantage for high Re flows. The Gradient Diffusion Hypothesis was not used at any point, thereby eliminating scope of any error that are known to arise from the use of this hypothesis in reactive flows (Libby and Bray, 1980).

From the computational effort standpoint, the PDF calculations were about twice as slow as compared to the ARSM calculations and four times slower than the k-ϵ calculations. This information, although discouraging, needs further clarification. The advantage of stochastic methods really lie in the context of reactive flows or for situations where the accuracy of the flow problem requires use of the differential Reynolds stress model, in which six additional non-linear partial differential equations need to be solved. Researchers in finite-volume computations will note that it typically takes enormous amount of computational effort to get the scalar transport equations to converge in a reactive flow situation. This is not the case for stochastic calculations. In fact, reactive flow calculations using finite-volume techniques are severely intractable if one were to incorporate finite-rate kinetics and radiation. PDF methods can easily account for these additional complexities without significant increase in computational effort. Thus, the importance of the proposed model and method lies in the context of heat transfer in reactive flow situations. Under such circumstances, the advantage of using stochastic models and methods truly become apparent.

Acknowledgment

The authors are grateful to the Applied Research Laboratory at Penn State for partial funding of this research, and for sharing their computer resources during the course of this work. The authors also wish to thank Prof. R.A. Antonia for providing the original data files used as comparison in some of the figures.

REFERENCES

Anand, M.S. and Pope, S.B., 1987, "Calculations of Premixed Turbulent Flames by PDF Methods", *Combustion and Flame*, Vol. 67, pp. 127–142.

Beguier, C., Dekeyser, I., and Launder, B.E., 1978, "Ratio of Scalar and Velocity Dissipation Time-Scales in Shear Flow Turbulence", *Physics of Fluids*, Vol. 21, No. 3, pp. 307–310.

De Boor, C., 1978, *A Practical Guide to Splines*, Springer-Verlag.

Dopazo, C., 1975, "Probability Density Function Approach for a Turbulent Axisymmetric Heated Jet. Centerline Evolution", *Physics of Fluids*, Vol. 18, No. 4, pp. 397–404.

Dreeben, T.D. and Pope, S.B., 1995, "PDF and Reynolds Stress Modeling of Near-Wall Turbulent Flows", *Tenth Symposium on Turbulent Shear Flows, The Pennsylvania State University*, pp. 21.

Durbin, P.A., 1993, "A Reynolds stress model for near-wall turbulence", *Journal of Fluid Mechanics*, Vol. 249, pp. 465–498.

Einstein, A., 1926, *Investigations on the Theory of Brownian Movement*, Methuen and Co. Ltd., London.

Hanjalic, K. and Launder, B.E., 1976, "Contribution towards a Reynolds-stress closure for low-Reynolds-number turbulence", *Journal of Fluid Mechanics*, Vol. 74, pp. 593–610.

Haworth, D.C. and Pope, S.B., 1987, "A PDF Modeling Study of Self-Similar Turbulent Free Shear Flows", *Physics of Fluids*, Vol. 30, pp. 1026–1044.

Janicka, J., Kolbe, W., and Kollmann, W., 1978, "The Solution of a PDF-Transport Equation for Turbulent Diffusion Flames", *Proc. Heat Trans. Fluid Mech. Inst.; Stanford University Press*.

Kader, B.A., 1981, "Temperature and Concentration Profiles in Fully Turbulent Boundary Layers", *Int. J. Heat Mass Transfer*, Vol. 24, No. 9, pp. 1541–1544.

Karlin, S.L. and Taylor, H.M., 1975, *A First Course in Stochastic Processes*, Academic Press, New York.

Karlin, S.L. and Taylor, H.M., 1981, *A Second Course in Stochastic Processes*, Academic Press, New York.

Launder, B.E., Reynolds, W.C., and Rodi, W., 1984, *Turbulence Models and their Applications*, Edition Eyrolles.

Leschziner, M.A., 1980, "Practical Evaluation of Three Finite Difference Schemes for the Computation of Steady-State Recirculating Flows", *Computer Methods in Applied Mechanics and Engineering*, Vol. 23, pp. 293–312.

Libby, P.A. and Bray, K.N.C., 1980, "Counter-Gradient Diffusion in Premixed Turbulent Flames", *AIAA Paper no. 80-0013*.

Lockwood, F.C. and Naguib, A.S., 1975, “The Prediction of the Fluctuations in the Properties of Free, Round-Jet, Turbulent, Diffusion Flame”, *Combustion and Flame*, Vol. 24, pp. 109–124.

Lyons, S.L., Hanratty, T.M., and McLaughlin, J.B., 1991, “Direct numerical simulation of passive heat transfer in a turbulent channel flow”, *Int. J. Heat Mass Transfer*, Vol. 34, pp. 1149–1161.

Mazumder, S. and Modest, M.F., 1996, “Boundary Conditions and an Efficient Pressure Algorithm for Internal Turbulent Flows using the PDF Method”, *Int. J. for Numerical Methods in Fluids*, (accepted; in press).

Pope, S.B., 1985, “PDF Methods for Turbulent Reactive Flows”, *Progress in Energy and Combustion Science*, Vol. 11, pp. 119–192.

Raithby, G.D., 1976, “A Critical Evaluation of Upstream Differencing Applied to Problems Involving Fluid Flow”, *Computer Methods in Applied Mechanics and Engineering*, Vol. 9, pp. 75–103.

Teitel, M. and Antonia, R.A., 1993, “Heat transfer in fully developed turbulent channel flow: comparison between experiment and direct numerical simulations”, *Int. J. Heat Mass Transfer*, Vol. 36, No. 6, pp. 1701–1706.

Tennekes, H. and Lumley, J., 1967, *A First Course in Turbulence*, MIT Press.

Warhaft, Z. and Lumley, J.L., 1978, “An Experimental Study of the Decay of Temperature Fluctuations in Grid-Generated Turbulence”, *J. Fluid Mech.*, Vol. 88, pp. 659–684.

Warhaft, Z., 1980, “An Experimental Study of the Effect of Uniform Strain on Thermal Fluctuations in Grid-Generated Turbulence”, *J. Fluid Mech.*, Vol. 99, pp. 545–573.

White, F.M., 1991, *Viscous Fluid Flow*, McGraw-Hill, Inc.